

Article

Analysis of Coalbed Methane Production Characteristics and Influencing Factors of No. 15 Coal Seam in the Shouyang Block

Bing Zhang^{1,2}, Wei Li¹, Gang Wang^{3,*}  and Xinglong Jiao¹

¹ Key Laboratory of Coalbed Methane Resources and Reservoir Formation Process, Ministry of Education, China University of Mining and Technology, Xuzhou 221008, China

² China United Coalbed Methane Corporation Ltd., Beijing 100011, China

³ College of Architecture & Civil Engineering, Shangqiu Normal University, Shangqiu 476000, China

* Correspondence: wgkdwb@163.com; Tel.: +86-370-2591111

Abstract: Based on the basic geological data and production data of coalbed methane wells in the Shouyang Block, the characteristics and influencing factors of coalbed methane well production were analyzed, and the primary controlling factors were identified by the grey correlation method. The results show that the average daily gas production of the coalbed methane wells in the study area for the single mining of No. 15 coal ranges from 0 to 604.34 m³/d, with an average of 116.82 m³/d. The overall average gas production is relatively low, with only 7 of the 42 wells having an average gas production greater than 200 m³/d. Gas production tends to increase as the gas content increases. There is a significant positive correlation between gas saturation and average gas production. Burial depth and coal seam thickness also show a positive correlation with average gas production. On the other hand, there is a negative exponential relationship between average gas production and critical desorption pressure. Permeability, as determined by well tests in the area, exhibits a negative correlation with the gas production of coalbed methane wells. The correlation between gas production and the mean three-dimensional stress is weak. As the fractal dimension D value of fractures increases, gas production decreases. A smaller difference in horizontal principal stress is more favorable for the formation of network fractures, facilitating reservoir fracturing and resulting in better reconstructive properties. Moreover, an increase in the sand–mud ratio leads to a decrease in average gas production. The correlation between fault fractal dimension and average gas production is weak. The grey correlation method was employed to determine the controlling factors of coalbed methane production in the study area, ranked from strong to weak, as follows: coal thickness > fracture fractal dimension D value > gas saturation > coal seam gas content > horizontal stress difference coefficient > permeability > critical desorption pressure > mean value of three-dimensional principal stress > coal seam burial depth > sand–mud ratio > fault fractal dimension.

Keywords: Shouyang Block; coalbed methane; gas production; influencing factors; grey correlation method



Citation: Zhang, B.; Li, W.; Wang, G.; Jiao, X. Analysis of Coalbed Methane Production Characteristics and Influencing Factors of No. 15 Coal Seam in the Shouyang Block. *Processes* **2023**, *11*, 3269. <https://doi.org/10.3390/pr11123269>

Academic Editors: Davide Dionisi, Junjian Zhang and Zhenzhi Wang

Received: 14 October 2023

Revised: 29 October 2023

Accepted: 17 November 2023

Published: 22 November 2023



Copyright: © 2023 by the authors. Licensee MDPI, Basel, Switzerland. This article is an open access article distributed under the terms and conditions of the Creative Commons Attribution (CC BY) license (<https://creativecommons.org/licenses/by/4.0/>).

1. Introduction

Coalbed methane, recognized as a clean and efficient unconventional energy source, has garnered significant global attention [1–5]. In recent years, some countries have made significant achievements in the production of coalbed methane. For example, the United States has become a major producer of coalbed methane and has extensive experience in the extraction and utilization of coalbed methane. Australia, China, Canada, and India have also made significant progress in this area. These countries have developed advanced drilling and mining technologies [6,7]. China, being the largest coal producer and consumer in the world, places great strategic importance on the development of coalbed methane resources [8,9]. There are several basins in China that contain coalbed methane resources, and most of the commercial development of coalbed methane is located in

the southern part of the Qinshui Basin and the eastern part of the Ordos Basin [10,11]. However, the development area is constrained, and the number of gas-producing coal seams is limited. Due to a lack of proper understanding of coalbed methane reservoirs, expected production rates often cannot be achieved [12]. In the southern part of the Qinshui Basin, less than one-fifth of the entire basin has been commercially developed for coalbed methane. In the past, commercial development has also focused on the No. 3 coal seam of the Shanxi Formation. To meet the demand for increasing production in the block, it is necessary to progressively mine multiple layers of coal [13]. The No. 9 and No. 15 coal seams of the Taiyuan Formation have good development conditions in the deep and northern parts of the basin, but there are only sporadic experimental projects and no actual resource development [14]. The Shouyang Block in the northern part of the Qinshui Basin, as an important coal production base in China, has abundant coalbed methane resources. Among them, the No. 15 coal seam has a large thickness, high gas content, and good sealing performance, which provides favorable conditions for coalbed methane development [15,16]. However, the development of coalbed methane in this block is still at an early stage. Previous studies have focused on various aspects, such as the characteristics of the No. 15 coal seam reservoir in the Shouyang Block, the enrichment patterns of coalbed methane [14,17,18], the hydrogeological control and production characteristics [19], the differences in coalbed methane well water production and the prediction of favorable areas [16,20], the identification of water sources for coalbed methane well discharge [21], and the feasibility of multi-layer combined mining of coalbed methane reservoirs [3,22,23]. However, there is a lack of systematic and in-depth research on gas production and its influencing factors. After fracturing and short-term production and drainage, the gas production of coalbed methane wells in the Shouyang Block is generally less than 500 m³/d [18], which seriously limits the development of coalbed methane resources in the Shouyang Block.

Gas production from coalbed methane wells is closely related to factors such as the degree of coalbed methane enrichment, reservoir permeability, reservoir modifiability, and the water content of coal-bearing formations. Therefore, this paper analyses the geological conditions for the coalbed methane development of No. 15 coal seam in the Shouyang Block, identifies the influencing factors and mechanisms of gas production, clarifies the strong or weak relationship between each influencing factor and gas production, and provides theoretical support and practical guidance for efficient coalbed methane development.

2. Geological Background

2.1. Structural Geological Conditions

The Shouyang Block is located in Shouyang County, eastern Shanxi Province, China, at the northern end of the Qinshui Basin, on the southern wing of the Yangqu–Yuxian latitudinal structural belt. The east and west sides of the block are controlled by the Taihang meridional structural belt and the Xinhua–Xia system structure, while the south is influenced by the Shouyang–Xiluo north–south structural belt. The structure is significantly influenced by the Yangqu–Yuxian latitudinal structural belt. The overall structure is monoclinic, with an east–west trend and southward inclination. Against this background, there are also some secondary folds and faults in different directions, and the structure in the area is relatively simple, with a general stratigraphic dip angle of 5–12 degrees (Figure 1).

2.2. Coal-Bearing Stratum

The Taiyuan Formation of the Upper Carboniferous is the main coal-bearing formation, with a thickness of 100.92–152.78 m and a general thickness of 123.00 m. The main mineable coal seam is No. 15. The lithology of the No. 15 coal roof predominantly consists of limestone, mudstone, sandy mudstone, and sandstone. The floor lithology mainly comprises sandy mudstone and mudstone. The sand body at the top of No. 15 coal eroded the lower coal-bearing strata during sedimentation, forming a coal-seam erosion zone in the northern

part of the study area (Figure 1). There are two groups of aquifers in the Shouyang Block, mainly sandstone or limestone aquifers adjacent to coal seams in the coal measures.

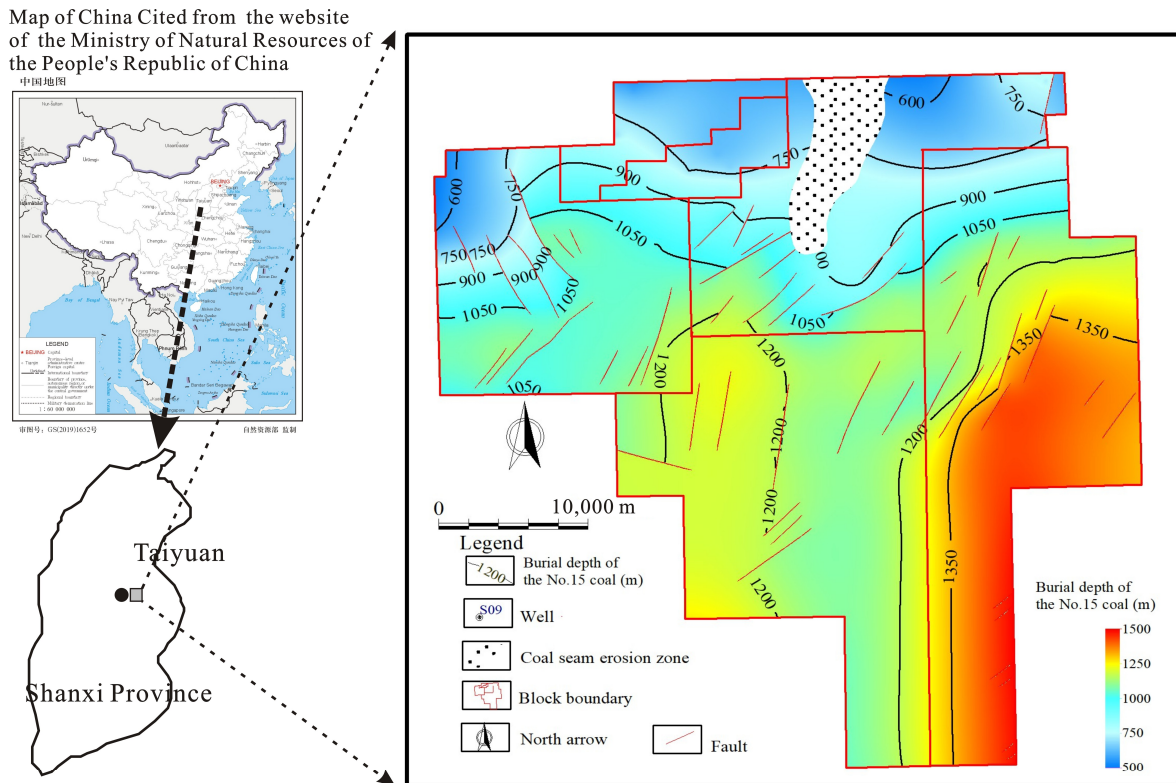


Figure 1. Location and structural geological map of the Shouyang Block.

3. Gas Production Characteristics

As of October 2022, the average daily gas production of the No.15 coal seam gas well in the study area ranges from 0 to 604.34 m³/d, with an average of 116.82 m³/d. Only seven out of 42 wells have an average gas production exceeding 200 m³/d, indicating a relatively low overall average gas production (Figure 2). The highest point of average gas production is mainly concentrated in the northeast of the Block, while the remaining areas demonstrate comparatively lower levels of gas production (Table 1; Figure 3).

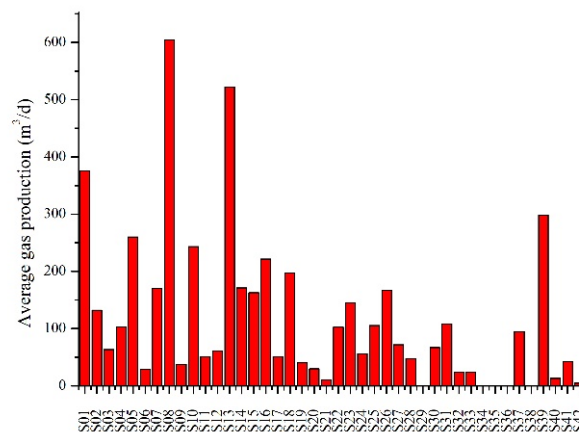


Figure 2. Column chart of average gas production of coalbed methane wells.

Table 1. Statistics of gas production of No. 15 coal single-mining coalbed methane wells in Shouyang Block.

Well	Average Gas Production (m ³ /d)	Buried Depth (m)	Coal Thickness (m)	Gas Content (m ³ /t)
S01	375.06	1115	3.7	12.14
S02	132.15	1415.7	3.2	19.08
S03	63.31	971.3	4.1	14.1
S04	103.25	1348.00	-	-
S05	259.97	668.90	3.50	15.00
S06	29.23	583.45	5.45	15.50
S07	170.69	1124.95	3.95	15.30
S08	604.34	1441.55	4.00	15.30
S09	37	668.90	3.50	15.00
S10	243.16	1418.75	4.35	15.21
S11	50.36	1226.40	4.65	16.00
S12	61.17	1355.30	4.15	20.00
S13	521.74	1166.30	3.80	16.45
S14	171.15	1238.75	3.90	16.51
S15	162.59	1164.50	5.15	14.90
S16	221.48	1261.10	4.70	16.35
S17	51.17	674.10	3.20	5.97
S18	197.1	637.20	3.90	5.57
S19	40.00	675.15	3.8	6.46
S20	30.00	859	3	5.03
S21	10.51	774.77	3.20	4.78
S22	102.32	711.30	4.10	4.58
S23	144.91	705.60	2.90	3.79
S24	56.11	880.10	3.70	3.15
S25	105.53	819.20	4.30	3.25
S26	166.96	852.60	4.60	2.83
S27	71.81	850.60	3.10	2.77
S28	47.06	-	-	-
S29	0	802.9	3.9	2.67
S30	66.73	997.27	6.67	2.56
S31	107.68	1237.65	5.45	16.5
S32	24.01	-	4.20	16.4
S33	23.98	-	-	-
S34	0	-	-	-
S35	0	1120.15	3.4	14.2
S36	0	1210.5	3.45	13.1
S37	94.55	674.65	4.7	-
S38	0	896.8	1.6	-
S39	298.84	654.2	2.6	-
S40	13.03	749.3	3.8	-
S41	42.71	756.55	4.2	-
S42	4.8	893.8	3.4	-

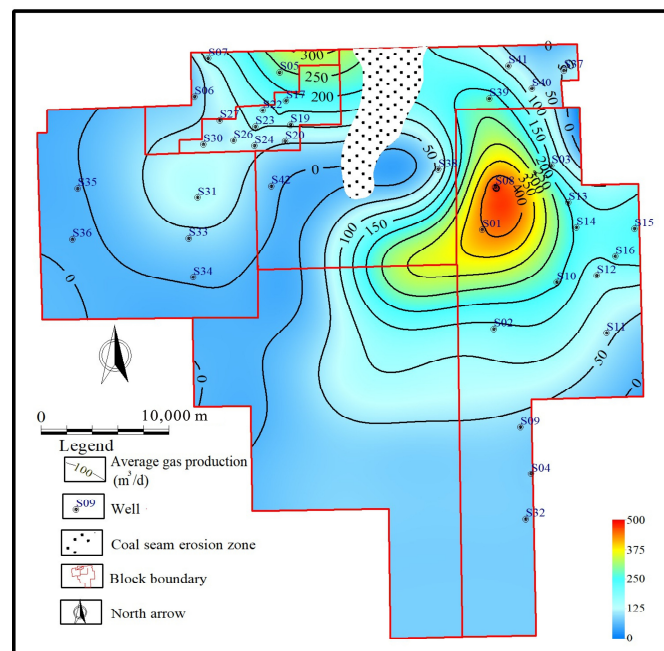


Figure 3. Distribution of average gas production in wells of No. 15 single mining.

4. Analysis of Influencing Factors

4.1. Gas Enrichment Factors

Coalbed methane enrichment is controlled by four primary factors: gas content, coal seam thickness, gas saturation, and critical desorption pressure. Coal seam thickness and gas content are the cornerstones of resource abundance. The gas saturation of coal seams reflects the degree of resource enrichment. The critical desorption pressure is commonly used to describe the release capacity of coalbed methane [24–28].

4.1.1. Gas Content and Gas Saturation

The gas content of No. 15 coal ranges from 2.56 to 20.00 m³/t, with an average of 10.95 m³/t. The enriched area is located in the eastern part of the block, with the lowest gas content observed in the northwest corner. The overall distribution exhibits a “high in the east and southeast, low in the central and lowest in the northwest” characteristic, with a gradual decrease and then increase from east to west. In addition, the change rate of gas content in the central region of the study area is relatively slow, while the change rate in the east and west is relatively fast (Figure 4). As the gas content increased, the gas production also showed an increasing trend, but the correlation was poor (Figure 5).

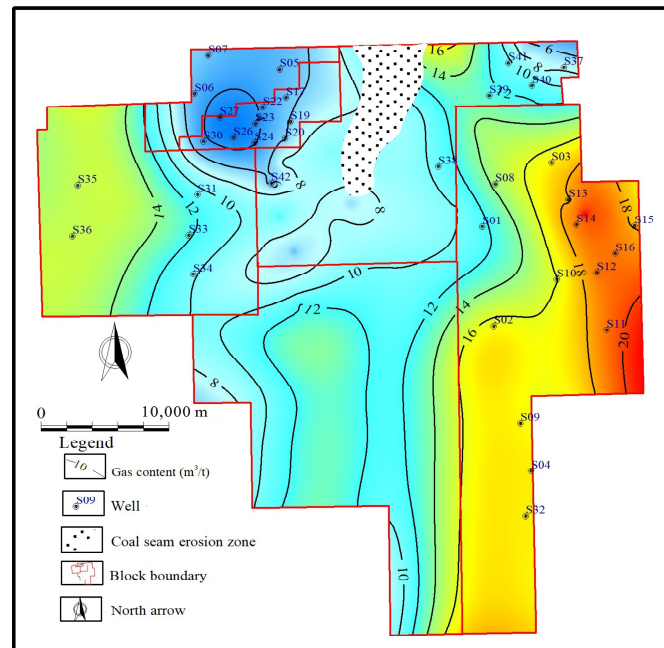


Figure 4. Contour map of gas content in No. 15 coal.

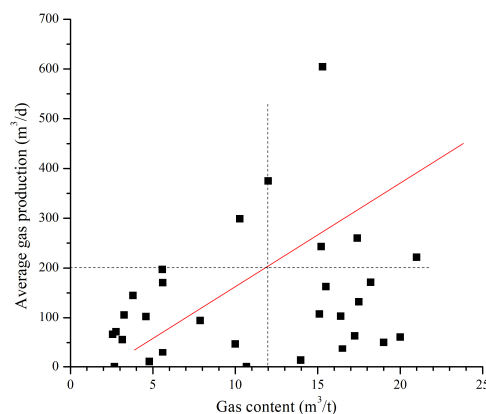


Figure 5. Relationship between gas content and average gas production in coal seams.

Gas saturation represents the adsorption “fullness” of adsorbed gas, which directly affects the production and recoverable reserves of coalbed methane, as well as the difficulty of desorption and depressurization in coalbed methane extraction. The gas saturation of No. 15 coal is relatively low, ranging from 0.22 to 0.68, with an average of 0.43 (Table 2). Gas saturation in the region shows a gradually increasing trend from north to south, with relatively high gas saturation on both sides of the western and eastern regions, especially in the southern region where high values appear, and relatively low gas saturation in the central and northern regions. The higher the gas saturation, the lower the pressure drop required for desorption and production of adsorbed gas. The shorter the time of the saturated water single-phase flow stage experienced by coalbed methane wells, the more favorable it is for coalbed methane wells to see gas in advance, and the higher the gas production [24,25]. There is a significant positive correlation between gas saturation and average gas production (Figures 6 and 7).

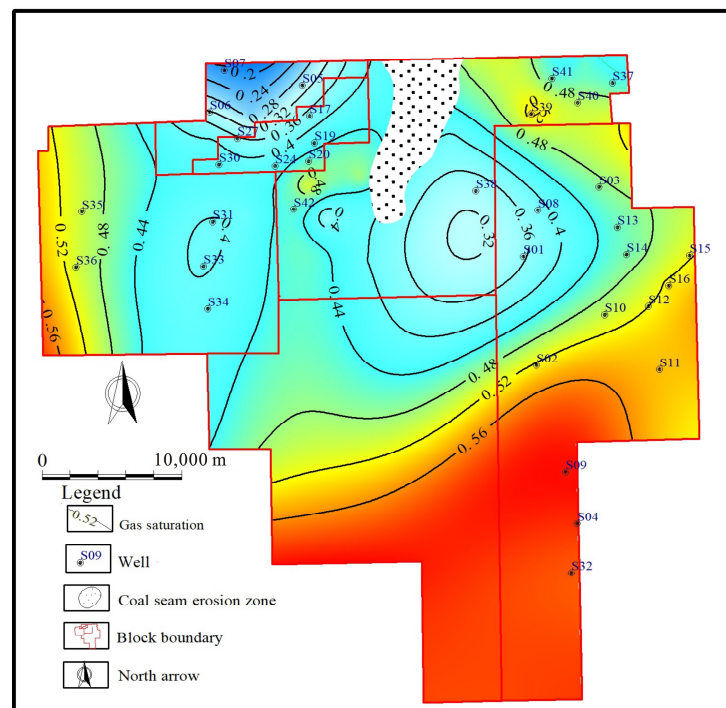


Figure 6. Contour map of gas saturation of No. 15 coal.

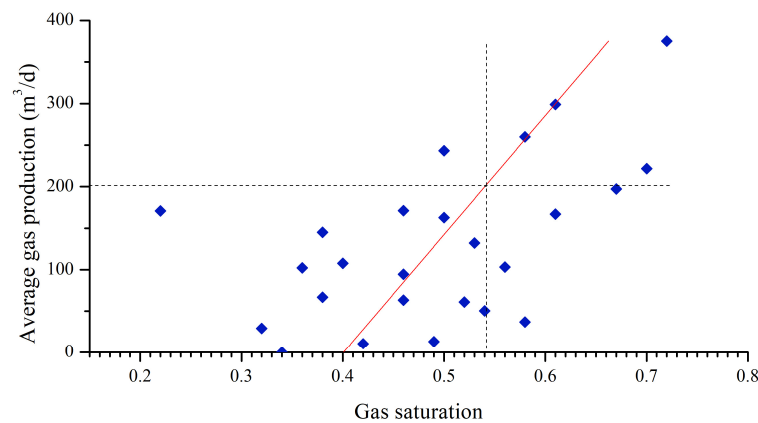


Figure 7. Relationship between gas saturation and average gas production.

Table 2. Statistics of various parameters of coalbed methane wells.

Well	Fractal Dimension D Value of Fracture	Fault Fractal Dimension Value	Sand–mud Ratio	Permeability (mD)	Gas Saturation	Critical Desorption Pressure (MPa)	Maximum Horizontal Principal Stress (MPa)	Minimum Horizontal Principal Stress (MPa)	Vertical Principal Stress (MPa)	Horizontal Stress Difference Coefficient (MPa)	Mean Value of Three-Dimensional Principal Stress (MPa)
S01	1.74	0.78	0.68	0.20	0.36	0.45	28.02	26.87	26.84	0.04	27.24
S02	1.60	0.90	0.42	0.15	0.53	2.35	24.00	22.50	25.00	0.07	23.83
S03	1.68	0.70	0.54	0.30	0.46	2.55	23.80	22.00	28.00	0.08	24.60
S06	1.75	0.20	1.20	1.80	0.32	1.14	18.50	14.00	20.00	0.32	17.50
S07	1.70	0.20	1.34	0.62	0.22	1.23	18.50	14.50	21.00	0.28	18.00
S08	1.74	0.90	0.63	0.30	0.38	0.71	25.50	21.00	23.50	0.21	23.33
S09	1.75	0.20	1.05	0.10	0.58	2.62	30.11	26.32	28.42	0.14	28.28
S10	1.70	0.83	1.00	0.10	0.50	0.25	15.44	12.92	23.34	0.20	17.23
S11	1.71	1.00	1.80	0.05	0.54	3.67	17.18	13.21	33.06	0.30	21.15
S12	1.74	0.62	1.85	0.05	0.52	3.00	17.50	15.00	29.00	0.17	20.50
S13	1.77	0.79	0.77	0.28	0.46	2.80	22.00	21.50	29.00	0.02	24.17
S14	1.78	0.70	0.81	0.46	0.50	1.00	25.00	23.80	33.00	0.05	27.27
S15	1.79	0.80	2.23	0.30	0.68	0.49	25.00	23.80	33.00	0.05	27.27
S17	1.79	0.20	1.04	0.50	0.42	1.68	20.05	17.50	15.83	0.15	17.79
S18	1.81	0.30	0.35	0.32	0.36	0.78	16.44	17.89	18.13	0.21	17.49
S19	1.84	0.94	0.44	0.52	0.38	1.45	16.24	16.77	19.69	0.11	17.57
S20	1.82	0.81	3.00	0.21	0.36	1.70	25.45	24.39	20.68	0.04	23.51
S21	1.82	0.90	3.12	0.20	0.32	1.80	20.35	17.57	18.38	0.16	18.77
S22	1.80	0.70	0.41	0.40	0.50	1.30	18.17	17.14	21.03	0.06	18.78
S23	1.77	0.65	1.52	1.00	0.36	1.30	17.46	12.95	20.37	0.35	16.93
S25	1.81	0.60	2.10	0.88	0.40	1.45	19.50	17.00	21.00	0.15	19.17
S26	1.62	0.50	2.50	1.50	0.38	1.46	22.00	18.00	25.71	0.22	21.90
S27	1.78	0.50	3.00	1.05	0.40	1.09	20.00	13.80	21.80	0.45	18.53
S29	1.63	0.40	4.80	1.00	0.50	2.50	19.50	15.50	21.40	0.26	18.80
S31	1.85	0.80	2.20	1.43	0.46	0.71	13.17	10.23	20.45	0.29	14.62
S32	1.71	0.84	1.24	0.25	0.34	1.27	18.20	15.67	19.43	0.16	17.77

4.1.2. Coal Thickness and Burial Depth

The greater the burial depth, the higher the geostress, and the lower the permeability of the coal reservoir [29,30]. The gas content increases with increasing burial depth within the critical depth range [31]. The burial depth of No.15 coal ranges from 583.45 m to 1441.55 m, with an average of 963.22 m. The coal thickness ranges from 1.60 to 6.67 m, with an average of 3.98 m. The high thickness areas are mainly distributed in the eastern and western strips of the block, with local areas exceeding 6.5 m. The areas with coal thickness exceeding 4.8 m are distributed in the western and southern parts of the study area, while the central part of the Shouyang block shows the thinnest coal thickness of less than 2 m (Figure 8). There is a positive correlation between coal seam thickness and average gas production. With increasing burial depth and coal thickness, the average gas production exhibits a significant increasing trend (Figures 9 and 10).

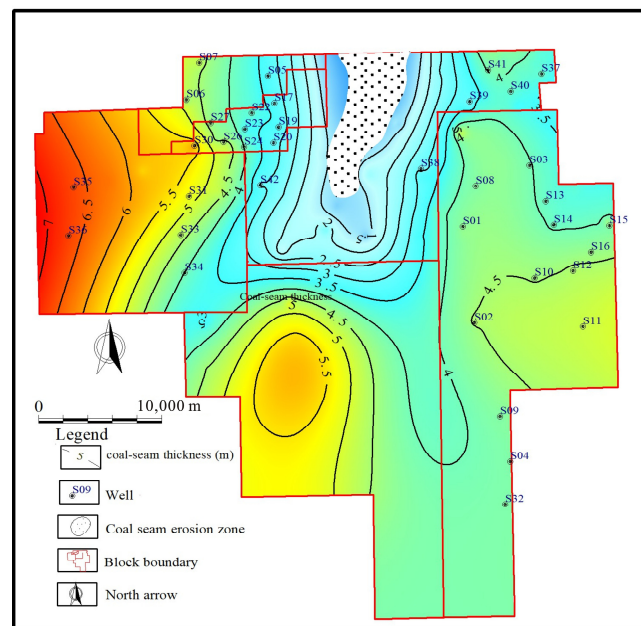


Figure 8. Contour map of coal thickness.

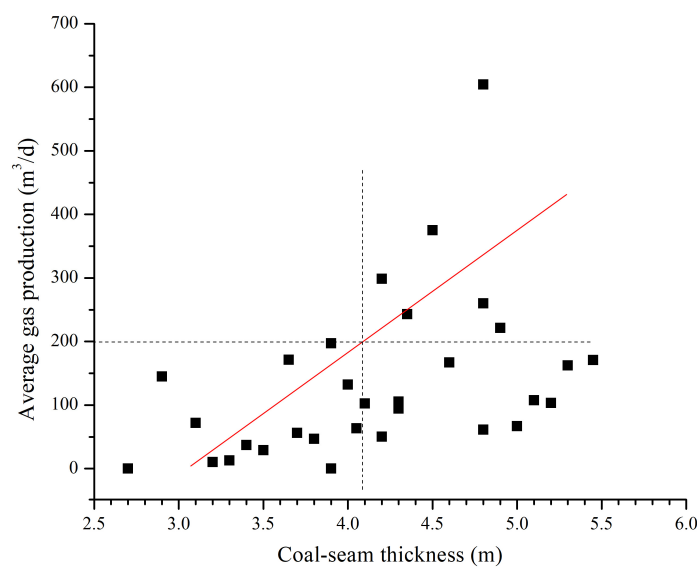


Figure 9. Relationship between coal seam thickness and average gas production.

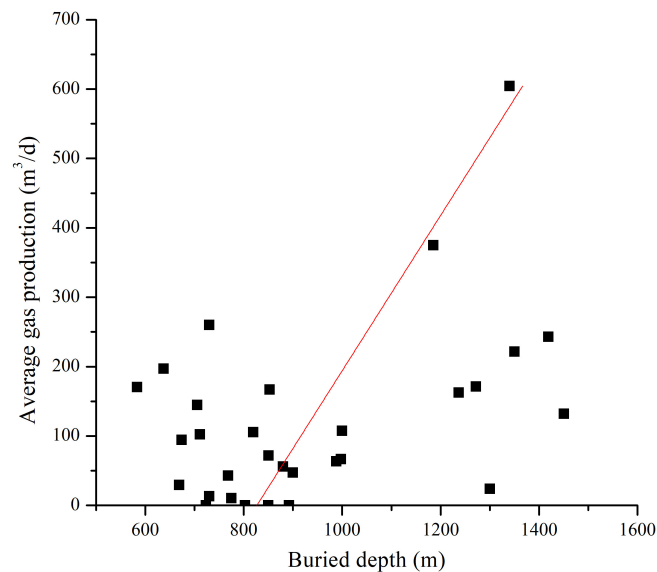


Figure 10. Relationship between coal seam burial depth and average gas production.

4.1.3. Critical Desorption Pressure

Coalbed methane wells utilize surface suction to enhance the production pressure differential, stimulate coal seam water production, reduce coal seam pressure, and ultimately achieve the goal of reducing the coal seam pressure below the critical desorption pressure, leading to continuous and stable gas production from coal seams [25]. The critical desorption pressure in the study area ranges from 0.25 to 3.67 MPa, with an average of 1.57 MPa. There is a negative exponential relationship between average gas production and critical desorption pressure (Figure 11).

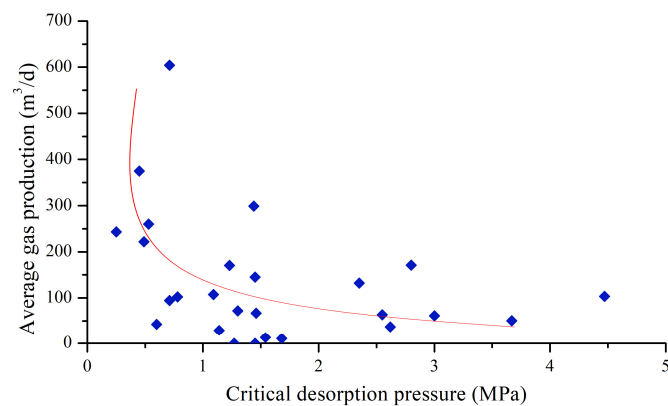


Figure 11. Relationship between critical desorption pressure and average gas production.

4.2. Permeability Factors

Coal seam “permeability” is the primary factor affecting coalbed methane production, and the permeability involves the conductivity of coal seams. Ground stress affects the distribution of coal seam fractures and the permeability of coal seams, which in turn affects the gas production of coalbed methane wells [29,32,33]. The fractal dimension D value of the fracture reflects the degree of fracture enrichment [34]. The permeability of the coal seams determines the strength of the coalbed methane transport capacity [27].

4.2.1. Permeability

The permeability data of the study area primarily rely on injection pressure drop tests. The permeability of coal seam 15 ranges from 0.015 to 1.80 mD, with an average of 0.54 mD.

The permeability of well tests in this area is negatively correlated with the average gas production of coalbed methane wells (Figure 12).

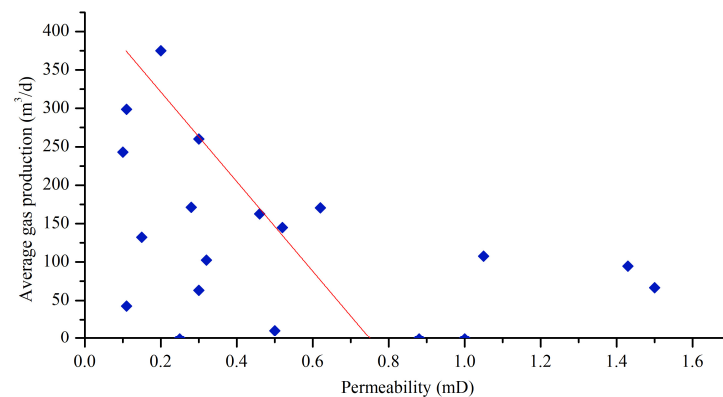


Figure 12. Relationship between permeability and average gas production.

4.2.2. Mean Value of Three-Dimensional Principal Stress

The maximum horizontal principal stress of No.15 coal in the study area ranges from 5.29 to 32 MPa, with an average of 21.6 MPa. The minimum horizontal principal stress ranges from 8.21 to 31.37 MPa, with an average of 18.99 MPa. Additionally, the vertical principal stress ranges from 6.67 to 22.75 MPa, with an average of 15.28 MPa.

Ground stress affects the shape, length, and degree of opening and closing of fractures. Fractures tend to close more easily and exhibit lower permeability and gas production when subjected to higher mean values of three-dimensional stress [29]. The correlation between the gas production of coal seams in the study area and the mean value of the three-dimensional stress is poor, indicating that gas production is greatly influenced by other factors (Figure 13).

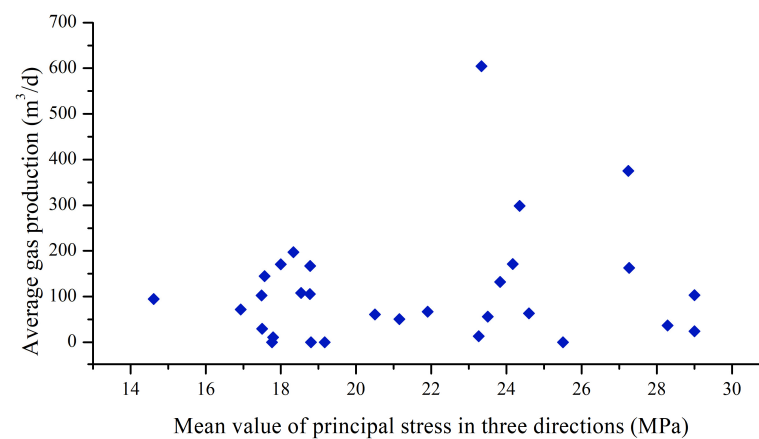


Figure 13. Relationship between the mean value of three-dimensional principal stress and average gas production.

4.2.3. Fractal Dimension D Value of Fracture

By utilizing the R/S fractal method to analyze the natural gamma logging data, the Hurst index for each well was obtained, and the corresponding D value was calculated [34]. The distribution of D values ranges from 1.61 to 1.89. As the fractal dimension D value of fractures increases, the gas production decreases. This finding suggests that a higher degree of coal structure fracturing corresponds to lower gas production from the coal seam (Figure 14).

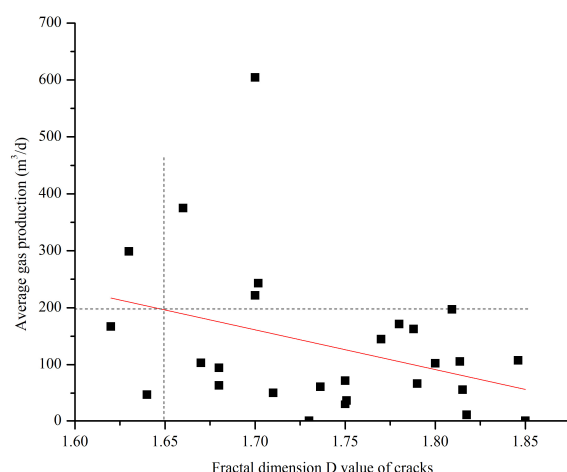


Figure 14. Relationship between fractal dimension D of fractures and average gas production.

4.3. Fracturing Factors

The initiation and extension of fracturing cracks must overcome not only the tensile strength of the rock, but also the constraints of the geological stress. The difference in geological stress will have a significant effect on fracture initiation. The smaller the difference in horizontal principal stress, the more favorable it is for the formation of network fracture, and the easier the reservoir can be fractured, resulting in better reconstructive properties. The horizontal stress difference coefficient refers to the ratio of the horizontal principal stress difference between two directions to the minimum horizontal principal stress [35]. The horizontal stress difference coefficient difference in the Shouyang block ranges from 0.01 to 0.45, with an average of 0.17 (Table 2). The correlation between the coal seam gas production and the horizontal stress difference coefficient in the study area is poor (Figure 15).

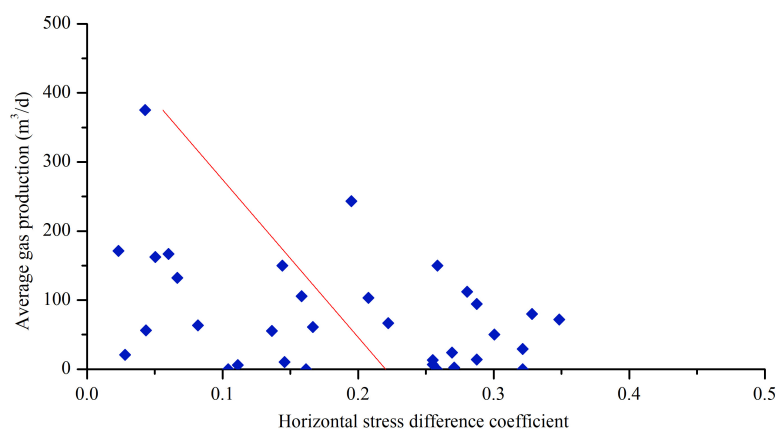


Figure 15. Relationship between the horizontal stress difference coefficient and average gas production.

4.4. Effluent Factors

In order to predict areas at risk of water outflow, it is beneficial to select reasonable water avoidance and gas recovery zones, which are influenced by sand–mud ratio and fault fractal dimension. Sandstone serves as a representative aquifer, whereas mudstone acts as an impermeable layer. The sand–mud ratio is an important indicator for describing the water abundance within the lithology. The fault fractal dimension quantifies the faults in a block, which have a significant impact on the communication of aquifers.

4.4.1. Sand–mud Ratio

The higher the sandstone content in the coal seam roof, the greater its thickness, and the greater its water abundance [36]. In this study, the sand–mud ratio serves as a primary indicator for evaluating the water abundance of the coal-seam roof aquifer. The smaller the sand–mud ratio, the more favorable it is for drainage and gas production [36]. The thickness of the sandstone and mudstone between the bottom of the No.15 coal and the K₃ limestone was calculated, and the sand–mud ratio was determined. The sand-to-mud ratio ranges from 0.09 to 18, with an average of 2.2. As the sand-to-mud ratio increases, there is a notable decrease in average gas production, demonstrating a strong and exponential correlation (Figure 16).

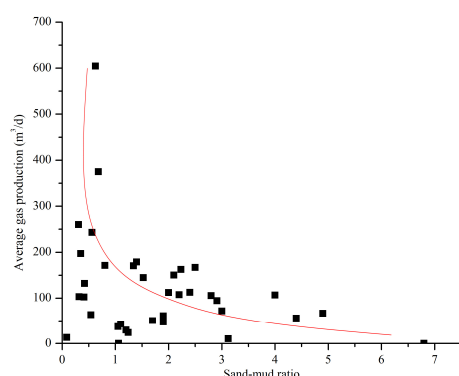


Figure 16. Relationship between sand–mud ratio and average gas production.

4.4.2. Fault Fractal Dimension

Fault structures are important channels for coalbed methane and water in the study area. To accurately quantify the complexity of these fault structures, similarity dimension parameters are employed for evaluation, and the fractal dimension of faults is calculated using the grid coverage method. For research objects exhibiting self-similarity, such as fault structures, the similarity dimension is calculated based on their division into N units, where each unit resembles the entirety of the object according to the similarity ratio, denoted as r [25]. The similarity dimension is defined as follows:

$$D_s = -\lg N(r) / \lg(r) \quad (1)$$

In Equation (1), D_s represents the similarity dimension, $N(r)$ represents the number of grids containing fault traces, and r represents the similarity ratio.

The fractal dimension of the faults in the study area ranges from 0 to 1.303, with an average of 0.71. However, the correlation between the fractal dimension of faults and average gas production is weak, indicating that other factors may have a more significant impact on gas production levels (Figure 17).

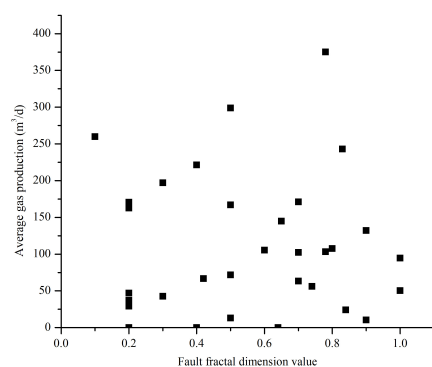


Figure 17. Relationship between fault fractal dimension and average gas production.

5. Discussion

The grey correlation analysis method is a statistical analysis approach that takes into account multiple factors. Grey correlation refers to the uncertain relationship between variables, and its main objective is to determine the degree of influence or contribution of factors to the main behavior. If two factors exhibit a consistent trend of changes, their correlation is considered significant. Conversely, if the trend differs significantly, the correlation is relatively weak [37,38]. Based on the previous analysis, 11 parameters including coal thickness, fracture fractal dimension D value, gas saturation, gas content, horizontal stress difference coefficient, permeability, critical desorption pressure, the mean value of three-dimensional principal stress, burial depth, sand–mud ratio, and fault fractal dimension were selected for grey correlation analysis. The correlation coefficient between each factor and average gas production was calculated to determine the primary and secondary levels of influence for each factor. The specific calculation steps are outlined as follows [39]:

(1) Determine the comparison sequence and reference sequence

Due to the varying level of detail in the parameters of each coalbed methane well in the study area, the reference sequence for this calculation is the average gas production of 32 wells extracted from No. 15 coal in Shouyang Block. The above 11 parameters corresponding to 32 wells is the comparison sequence. Set the reference sequence as $\{x_i(n)\}$ and the comparison sequence as $\{y_i(n)\}$, where the variation range of i is 1–11, and the variation range of n is 1–32;

(2) Depersonalization and normalization of parameters

Due to the different physical meanings, numerical ranges, and units of each evaluation indicator, in order to facilitate comparison between various parameters, it is necessary to process each parameter into dimensionless data and convert it into a number between 0 and 1.

(3) Determine correlation coefficient

When $n = k$, the reference sequence is represented as $\{x_i(k)\}$, and the comparison sequence is represented as $\{y(k)\}$, with their correlation coefficients $\varepsilon_i(k)$ calculated using the following formula:

$$\varepsilon_i(k) = \frac{\Delta_i(\min) + \rho\Delta_i(\max)}{\Delta_i(k) + \rho\Delta_i(\max)} \quad (2)$$

In Equation (2), $\Delta_i(\max)$ and $\Delta_i(\min)$ represent the maximum and minimum absolute values of the difference between the reference sequence and the comparison sequence, respectively; $\Delta_i(k)$ is the absolute value of the difference between the two when $n = k$, i.e., $\Delta_i(k) = y(k) - x_i(k)$; and ρ The resolution coefficient is usually 0.5.

(4) Calculate the correlation coefficient

Calculate the average correlation coefficient between the comparison sequence and the reference sequence at different points, and calculate it using the following formula.

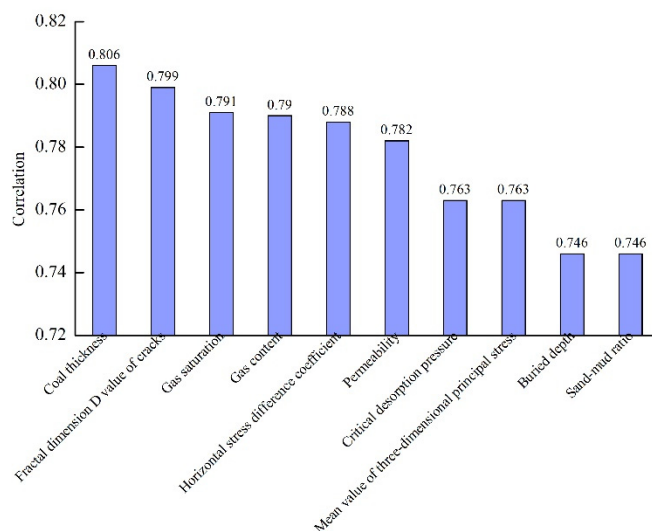
$$R_i = \frac{1}{n} \sum_{k=1}^n \varepsilon_i(k) \quad (3)$$

Calculate the degree of correlation between each parameter and daily gas production according to Equation (3), and sort them according to their relationship.

Based on the correlation coefficient comparison results, the factors influencing coalbed methane production in the study area can be ranked from strong to weak, as follows: coal thickness > fracture fractal dimension D value > gas saturation > gas content > horizontal stress difference coefficient > permeability > critical desorption pressure > mean value of three-dimensional principal stress > burial depth > sand–mud ratio > fault fractal dimension (Table 3; Figure 18).

Table 3. Correlation and ranking statistics between comparative sequences and reference sequences.

Factors Affecting Gas Production	Coal Thickness	Fracture Fractal Dimension D Value	Gas Saturation	Gas Content	Horizontal Stress Difference Coefficient	Permeability
Correlation	0.806	0.799	0.791	0.79	0.788	0.782
Factors affecting gas production	Critical desorption pressure	Mean value of three-dimensional principal stress	Burial depth	Sand–mud ratio	Fault fractal dimension	
Correlation	0.763	0.763	0.746	0.746	0.723	

**Figure 18.** Ranking of factors influencing gas production.

In coalbed methane development, factors such as coal thickness, fracture fractal dimension D value, gas saturation and gas content can be prioritized to achieve efficient development. According to Figures 5, 7, 9 and 14, when the coal thickness is greater than 4.1 m, the fracture fractal dimension D value is less than 1.65, the gas saturation is greater than 0.54, the gas content is greater than 12 m³/t, and the average gas production will reach over 200 m³/d.

6. Conclusions

(1) The characteristics of coalbed methane production in the Shouyang Block have been identified. The average daily gas production of coalbed methane wells in the study area ranges from 0 to 604.34 m³/d, with an average of 116.82 m³/d. The overall average gas production is relatively low, with only 7 of the 42 wells having an average gas production greater than 200 m³/d. The highest average point is mainly concentrated in the northeast of the block, while the remaining areas exhibited relatively lower production levels.

(2) Gas production tends to increase as the gas content increases. There is a significant positive correlation between gas saturation and average gas production. Burial depth and coal seam thickness also show a positive correlation with average gas production. On the other hand, there is a negative exponential relationship between average gas production and critical desorption pressure. Permeability, as determined by well tests in the area, exhibits a negative correlation with the gas production of coalbed methane wells. The correlation between gas production and the mean three-dimensional stress is weak. As the fractal dimension D value of fractures increases, gas production decreases. A smaller difference in horizontal principal stress is more favorable for the formation of network fractures, facilitating reservoir fracturing and resulting in better reconstructive properties. Moreover, an increase in the sand–mud ratio leads to a decrease in average gas production. The correlation between fault fractal dimension and average gas production is weak.

(3) The grey correlation method was employed to determine the controlling factors of coalbed methane production in the study area, ranked from strong to weak, as follows: coal thickness > fracture fractal dimension D value > gas saturation > coal seam gas content > horizontal stress difference coefficient > permeability > critical desorption pressure > mean value of three-dimensional principal stress > coal seam burial depth > sand–mud ratio > fault fractal dimension.

Author Contributions: Conceptualization, B.Z. and W.L.; methodology, W.L., G.W. and X.J.; software, W.L., G.W. and X.J.; investigation, B.Z., W.L. and X.J.; writing—original draft preparation, W.L. and G.W.; writing—review and editing, G.W.; project administration, B.Z.; funding acquisition, B.Z. All authors have read and agreed to the published version of the manuscript.

Funding: This research was funded by the Announcement Project of Shanxi Province, China, grant number 20201101002.

Data Availability Statement: The data used to support the findings of this study are included within the article.

Conflicts of Interest: Author Bing Zhang was employed by the company China United Coalbed Methane Corporation Ltd. The remaining authors declare that the research was conducted in the absence of any commercial or financial relationships that could be construed as a potential conflict of interest.

References

1. Wang, Y.Y.; Bao, Y.; Hu, Y.L. Recent progress in improving the yield of microbially enhanced coalbed methane production. *Energy Rep.* **2023**, *9*, 2810–2819. [[CrossRef](#)]
2. Du, S.; Wang, M.; Yang, J.; Zhao, Y.; Wang, J.; Yue, M.; Xie, C.; Song, H. An enhanced prediction framework for coalbed methane production incorporating deep learning and transfer learning. *Energy* **2023**, *282*, 128877. [[CrossRef](#)]
3. Liang, S.; Liang, Y.; Elsworth, D.; Yao, Q.; Fu, X.; Kang, J.; Hao, Y.; Wang, M. Permeability evolution and production characteristics of inclined coalbed methane reservoirs on the southern margin of the Junggar Basin, Xinjiang, China. *Int. J. Rock Mech. Min. Sci.* **2023**, *171*, 105581. [[CrossRef](#)]
4. Sadegh, K.; Pejman, T.; Hamed, L.R. A review of experimental and numerical modeling of digital coalbed methane: Imaging, segmentation, fracture modeling and permeability prediction. *Int. J. Coal Geol.* **2020**, *228*, 103552.
5. Ritter, D.J.; Vinson, D.S.; Barnhart, E.P.; Akob, D.M.; Fields, M.W.; Cunningham, A.B.; Orem, W.H.; McIntosh, J.C. Enhanced microbial coalbed methane generation: A review of research, commercial activity, and remaining challenges. *Int. J. Coal Geol.* **2015**, *146*, 28–41. [[CrossRef](#)]
6. Freij-Ayoub, R. Opportunities and challenges to coal bed methane production in Australia. *J. Pet. Sci. Eng.* **2012**, *88–89*, 1–4. [[CrossRef](#)]
7. Sujoy, C.; Debadutta, M.; Tarkeshwar, K.; Gopinath, H. Thermodynamics, kinetics and modeling of sorption behaviour of coalbed methane—A review. *J. Unconv. Oil Gas Resour.* **2016**, *16*, 14–33.
8. Wang, G.; Qin, Y.; Xie, Y.W. Geochemical Characteristics of Coal in the Taiyuan Formation in the Center and North of the Xishan Coalfield. *Energies* **2022**, *15*, 8025. [[CrossRef](#)]
9. Jing, W.; Zhou, J.; Yuan, L.; Jin, R.; Jing, L. Deformation and Failure Mechanism of Surrounding Rock in Deep Soft Rock Tunnels Considering Rock Rheology and Different Strength Criteria. *Rock Mech. Rock Eng.* **2023**. [[CrossRef](#)]
10. Li, H.Y.; Lau, H.C.; Huang, S. China's coalbed methane development: A review of the challenges and opportunities in subsurface and surface engineering. *J. Pet. Sci. Eng.* **2018**, *166*, 621–635. [[CrossRef](#)]
11. Li, Z.; Liu, D.; Wang, Y.; Si, G.; Cai, Y.; Wang, Y. Evaluation of multistage characteristics for coalbed methane desorption-diffusion and their geological controls: A case study of the northern Gujiao Block of Qinshui Basin, China. *J. Pet. Sci. Eng.* **2021**, *204*, 108704. [[CrossRef](#)]
12. Achinta, B.; Subhash, S. A review on modern imaging techniques for characterization of nanoporous unconventional reservoirs: Challenges and prospects. *Mar. Pet. Geol.* **2021**, *133*, 105287.
13. Zhang, C.; Li, M.X.; Feng, S.R.; Hu, Q.J.; Qiao, M.P.; Wu, D.Q.; Yu, J.S.; Li, K.X. Reservoir properties and gas production difference between No.15 coal and No.3 coal in Zhengzhuang Block, southern Qinshui Basin. *Coal Geol. Explor.* **2022**, *50*, 145–153.
14. Jiang, W.; Zhang, P.; Li, D.; Li, Z.; Wang, J.; Duan, Y.; Wu, J.; Liu, N. Reservoir characteristics and gas production potential of deep coalbed methane: Insights from the no. 15 coal seam in shouyang block, Qinshui Basin, China. *Unconv. Resour.* **2022**, *2*, 12–20. [[CrossRef](#)]
15. Zhang, X.; Wang, R.Y. Study on occurrence features as well as exploration and development of coalbed methane in Shouyang North Block, Shanxi. *Coal Sci. Technol.* **2015**, *43*, 99–104.
16. Wang, J.; Kang, Y.; Jiang, S.; Zhang, S.; Ye, J.; Wu, J. Reasons for water production difference of CBM wells in Shouyang Block, Qinshui Basin, and prediction on favorable areas. *Nat. Gas Ind.* **2016**, *36*, 52–59.

17. Zhang, Y.S.; He, J.; Zhang, Y.F.; Duan, J.; Kang, L.; Wang, Z. Enrichment Law and Optimization of Coal Bed Methane Reservoir in Shouyang Block, Qinshui Basin. *China Pet. Chem. Stand. Qual.* **2022**, *42*, 124–126.
18. Zhu, H.Y.; Tang, X.H.; Liu, Q.Y.; Liu, S.; Zhang, B.; Jiang, S.; McLennan, J.D. McLennan. Permeability stress-sensitivity in 4D flow-geomechanical coupling of Shouyang CBM reservoir, Qinshui Basin, China. *Fuel* **2018**, *232*, 817–832. [[CrossRef](#)]
19. Du, F.; Ni, X.; Zhang, Y.; Wang, W.; Wang, K. Hydrological control mode and production characteristics of coalbed methane field in Shouyang block. *Coal Sci. Technol.* **2023**, *51*, 177–188. [[CrossRef](#)]
20. Lv, Y.; Liu, Y.; Wang, C.; Guo, G.; Zhu, X.; Jiang, R. Controls on High Water Production of CBM Wells in Shouyang Block, Qinshui Basin. *Geoscience* **2017**, *31*, 1088–1094.
21. Kang, Y.S.; Chen, J.; Zhang, B. Identification of aquifers influencing the drainage of coalbed methane wells in Shouyang exploration area, Qinshui Basin. *J. China Coal Soc.* **2016**, *41*, 2263–2272.
22. Wang, Z.Y.; Tang, S.H.; Sun, P.J.; Zheng, G. Feasibility Study of Multi-layer Drainage for Nos. 3 and 9 Coal Seams in Shouyang Block, Qinshui Basin. *Coal Geol. China* **2013**, *25*, 21–26.
23. Huang, L.; Hu, Q.; Guo, Y.; Zhou, J.H. Feasibility of Multiple-zone Production in CBM Reservoirs, Shouyang Block, Qinshui Basin. *Nat. Gas Technol. Econ.* **2017**, *11*, 21–24.
24. Zheng, A.; Wang, X.; Wang, X.; Wu, M.; Yuan, Y. The Effect of Coal Seam Gas saturation on CBM Well Productivity-A Case Study of Central Region of Hedong Area. *Procedia Eng.* **2011**, *26*, 1205–1213. [[CrossRef](#)]
25. Zhang, Z.G. *Controlling Factors of Productivity Difference of Coalbed Methane Wells in Eastern Yunnan and Western Guizhou*; China University of Mining and Technology: Xuzhou, China, 2022.
26. Lu, Y.Y.; Zhang, H.D.; Zhou, Z.; Ge, Z.L.; Chen, C.J.; Hou, Y.D.; Ye, M.L. Current status and effective suggestions for efficient exploitation of coalbed methane in China: A review. *Energy Fuels* **2021**, *35*, 9102–9123. [[CrossRef](#)]
27. Moore, T.A. Coalbed methane: A review. *Int. J. Coal Geol.* **2012**, *101*, 36–81. [[CrossRef](#)]
28. Li, C.; Yang, Z.; Chen, J.; Sun, H. Prediction of Critical Desorption Pressure of Coalbed Methane in Multi-coal Seams Reservoir of Medium and High Coal Rank: A Case Study of Eastern Yunnan and Western Guizhou, China. *Nat. Resour. Res.* **2022**, *31*, 1443–1461. [[CrossRef](#)]
29. Shen, J.; Qin, Y.; Li, Y.; Yang, Y.; Ju, W.; Yang, C.; Wang, G. In situ stress field in the FZ Block of Qinshui Basin, China: Implications for the permeability and coalbed methane production. *J. Pet. Sci. Eng.* **2018**, *170*, 744–754. [[CrossRef](#)]
30. Wang, G.; Xie, Y.; Chang, H.; Du, L.; Wang, Q.; He, T.; Zhang, S. Characteristics and Geological Impact Factors of Coalbed Methane Production in the Taiyuan Formation of the Gujiao Block. *Processes* **2023**, *11*, 2000. [[CrossRef](#)]
31. Qin, Y.; Shen, J. On the fundamental issues of deep coalbed methane geology. *Acta Pet. Sin.* **2016**, *37*, 125–136.
32. Wang, Z.; Fu, X.; Pan, J.; Deng, Z. Effect of N₂/CO₂ injection and alternate injection on volume swelling/shrinkage strain of coal. *Energy* **2023**, *275*, 127377. [[CrossRef](#)]
33. Pan, J.; He, H.; Li, G.; Wang, X.; Hou, Q.; Liu, L.; Cheng, N. Anisotropic strain of anthracite induced by different phase CO₂ injection and its effect on permeability. *Energy* **2023**, *284*, 128619. [[CrossRef](#)]
34. Hu, Z.Q. Application of R/S analysis in the evaluation of vertical reservoir heterogeneity and fracture development. *Exp. Pet. Geol.* **2000**, *04*, 382–386.
35. Song, M.S.; Liu, Z.; Zhang, X.C.; Wang, Y.; Li, J.; Yang, F. Fracability evaluation of tight reservoirs based on improved entropy analytic hierarchy process: Taking the Jurassic reservoirs of Well Z109 in the Junggar Basin as an example. *J. Geomech.* **2019**, *25*, 509–517.
36. Zhang, B. CBM Well Produced Water Source Identification and Favorable Block Prediction in Shouyang Area. *Coal Geol. China* **2016**, *28*, 67–73.
37. Huo, Z.B. Analysis on the Difference and Main Controlling Factors of Gas-Water Productivity of CBM Straight Wells in Zhengzhuang South Qinshui Basin. Master's Thesis, China University of Mining and Technology, Xuzhou, China, 2017.
38. Dang, F. *Analysis of Factors Influencing the Productivity of Coalbed Methane in Different Geological Units in Shizhuangnan Block, Qinshui Basin*; China University of Geosciences: Beijing, China, 2020. [[CrossRef](#)]
39. Han, W.L.; Wang, Y.B.; Ni, X.M.; Li, Y.; Tao, C.; Liu, Z.M.; Wu, X. Influence of normal development faults characteristics on the exploitation of vertical coal-bed methane wells: A case study of the Shizhuang Block in the south of Qinshui Basin. *J. China Coal Soc.* **2020**, *45*, 3522–3532.

Disclaimer/Publisher's Note: The statements, opinions and data contained in all publications are solely those of the individual author(s) and contributor(s) and not of MDPI and/or the editor(s). MDPI and/or the editor(s) disclaim responsibility for any injury to people or property resulting from any ideas, methods, instructions or products referred to in the content.